

# ANALYSIS OF RATE-BASED CONGESTION CONTROL ALGORITHMS FOR ATM NETWORKS

## — PART 2: INITIAL TRANSIENT STATE ANALYSIS —

Hiroyuki Ohsaki, Masayuki Murata, †Hiroshi Suzuki, †Chinatsu Ikeda and Hideo Miyahara

Department of Information and Computer Sciences  
Faculty of Engineering Science, Osaka University  
Toyonaka, Osaka 560, Japan

†C&C System Research Laboratories  
NEC Corporation  
Kawasaki, Kanagawa 216, Japan

**Abstract** — Rate-based congestion control is effective and still simple for traffic management in ATM networks. As one of practical realization schemes, Enhanced Proportional Rate Control Algorithm (EPRCA) has recently been proposed and adopted as a standard by the ATM Forum. While EPRCA can offer a desirable feature in steady state, the queue length considerably grows when the active number of connections on the link becomes large, which is so called a “large VC’s problem.” In particular, when the large number of VC’s starts cell transmission at same time, the rate-control does not work well. We present an analytic result to give a deep insight into this problem for three types of switches suggested in EPRCA. Further, we demonstrate that a prioritized switch which can limit a maximum queue length at an appropriate level.

### I. INTRODUCTION

Congestion control plays an essential part for efficient traffic management in ATM networks. Recently, rate-based congestion control is adopted by the ATM Forum for ABR (Available Bit Rate) service because of its simplicity for implementation and scalability from local area to wide area networks. In rate-based congestion control, the cell transmission rate at source end system is controlled by feedback information from the network. The source end system increases cell transmission rate if the network is not congested. Once the network is congested, the source end system decreases its cell transmission rate after it receives congestion indication. For more detailed description of rate-based congestion control for ATM networks, refer to [1, 2].

Several analytic studies for the rate-based control scheme have already been made [3, 4, 5]. For example, Yin et al. analyzed a dynamical behavior of the rate-based congestion control with timer-based approach [5]. In their model, the source end system changes its cell transmission rate regularly at every fixed time interval. However, it has already been found that this approach causes problems in some situations [6]. Henceforth, an improved rate control algorithm called Enhanced Proportional Rate Control Algorithm (EPRCA) is recently proposed in [7], which has been adopted by the ATM Forum as a standard for the rate-based congestion control scheme for ABR service in ATM networks.

EPRCA defines source and destination end systems’ beha-

avior, and suggests three types of switches, EFCI bit setting switch (EFCI), Binary Enhanced Switch (BES) and Explicit Down Switch (EDS). Each switch has different functions against network congestion. In the companion paper [1], we have introduced and analyzed three types of switches in the above as well as the prioritized switch which has a capability to give priority service to control cells over data cells. While the analysis presented in [1] exhibits the effectiveness of EPRCA switches in steady state, a careful analytic treatment is necessary when the large number of connections share the link. Since the aggregate rate of the active connections is increased rapidly in such a circumstance, the queue length tends to be unacceptably large. This tendency becomes distinguishable when multiple connections start cell transmission at same time. This is known as a “large VC’s problem”, and is one of serious problems against effective rate-based congestion control, which is our main subject of the current paper.

In this paper, we analyze an initial transient behavior of the above-mentioned switches by a similar approach taken in [1]. Different from the one in [1], however, we explicitly model the emission time of RM cells to explore the initial transient behavior of the system. By assuming that all connections begin their cell transmission simultaneously, we will show a dynamical behavior of EPRCA and a minimum buffer requirement for each of switches.

The rest of this paper is organized as follows. Our analytic model for EPRCA is presented briefly in Section II. Section III is devoted to the analysis of three switches. Our concluding remarks are presented in Section IV.

### II. ANALYTIC MODEL

In this paper, we provide the initial transient analysis for three types of EPRCA switches using the same model as in our companion paper [1]. For details of our analytic model and definitions of parameters, refer to [1].

In [1], we have analyzed evolution of  $ACR(t)$  (allowed cell rate for each connection), and  $Q(t)$  (queue length at the switch) in steady state. As shown in that paper, as the number of connections becomes large, the queue length tends to be extremely large especially in the case of the EFCI switch. This tendency becomes unacceptable in the case where the large number of

connections starts cell transmission at same time. It depends on  $IMR$  and  $ICR$ , which are initial values of  $MACR$  and  $ACR$ , respectively, and our analysis in the current paper will exhibit the effect of those parameter values on the initial transient behavior of the switches.

Since  $ICR$  can be chosen freely, one may consider that  $ICR$  should be set to be small enough so that the queue length does not become large. As shown in the numerical examples, it is true if one can know the number of active connections ( $N_{VC}$ ) in advance. However, in the actual network environment, it may be difficult. Furthermore, a smaller value of fixed  $ICR$  cannot achieve high utilization of the link when  $N_{VC}$  is small. In this paper, we provide the analysis of an initial transient behavior of rate-based congestion control for given  $N_{VC}$  and  $ICR$  to exploit the suggestive control parameters by assuming that (1) the switch has infinite capacity of the buffer, and that (2) the source end system always has cells to transmit. Therefore,  $ACR(t)$  is equivalent to the actual cell transmission rate. Besides three types of switches, we will also treat a prioritized EDS switch (PEDS). As will be shown in numerical examples, the maximum queue length can be considerably decreased by PEDS.

### III. INITIAL TRANSIENT STATE ANALYSIS

When several connections start their cell transmission at the same time, queue length at the switch grows considerably unless control parameters such as  $ICR$  (Initial Cell Rate) are set properly. This tendency becomes unacceptable as the number of connections is large. This is known as a ‘‘large VC’s problem’’. It can be evaluated by the initial transient analysis, which is presented in this section. The difference between the approach taken in the previous paper [1] and the one in the current paper is that in the initial transient analysis, the transmission time of RM cells should be carefully treated in the analysis to investigate the initial behavior of queue lengths at the switch. Especially, in the case of EDS switches, transmission times of RM cells are explicitly taken into account as will be presented in Subsection III-C.

#### A. EFCI Switch

In this subsection, we analyze the initial transient behavior of the allowed cell rate  $ACR(t)$  and the queue length  $Q(t)$  of the EFCI switch for a given  $ICR$  to show that an appropriate choice of  $ICR$  plays an important role for achieving effective control while suppressing the maximum queue length to an appropriate value. The latter is important for buffer-dimensioning in designing ATM switches.

##### 1) Derivation of $ACR(t)$ :

Figure 1 show pictorial views of  $ACR(t)$  and  $Q(t)$  of the EFCI switch in the initial transient state for  $ICR < BW/N_{VC}$ . The evolution of  $ACR(t)$  and  $Q(t)$  is classified into two categories according to the relation between  $ICR$  and  $BW/N_{VC}$ . To see this, we will derive  $ACR(t)$  and  $Q(t)$  from now on. Here, we should note that a more rigorous treatment is required regarding the above classification because it should also be affected by other parameters as will be shown in the below.

We first divide  $ACR(t)$  into phases, each of which has a different form dependent on the congestion status of the switch.

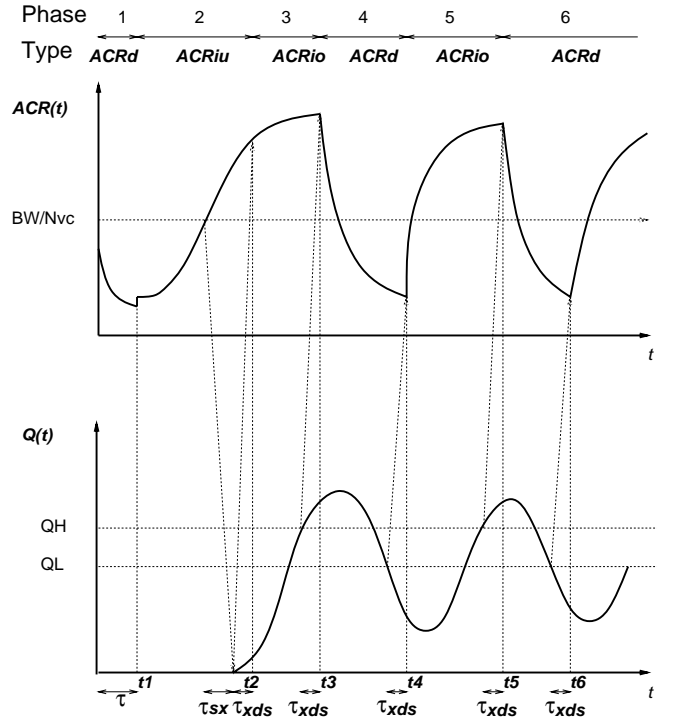


Fig. 1: Pictorial View of EFCI Switch ( $ICR < BW/N_{VC}$ ).

There are three types of  $ACR(t)$ .

- Type 1:  $ACR_d(t)$   
 $ACR(t)$  is decreased exponentially.
- Type 2:  $ACR_{iu}(t)$   
 $ACR(t)$  is increased and the offered load to the link is below its capacity  $BW$ .
- Type 3:  $ACR_{io}(t)$   
 $ACR(t)$  is increased and the offered load to the link is beyond its capacity  $BW$ .

In the case of  $ICR < BW/N_{VC}$ ,  $ACR_d(t)$ ,  $ACR_{iu}(t)$ ,  $ACR_{io}(t)$  appears in this order (see Fig. 1). Then,  $ACR_d(t)$  and  $ACR_{io}(t)$  are repeated. On the other hand, a cycle consisting of  $ACR_d(t)$  and  $ACR_{io}$  is repeated in the case of  $ICR > BW/N_{VC}$ . Let us denote  $ACR_i(t)$  and the corresponding  $Q_i(t)$  as  $ACR(t)$  and  $Q(t)$  of Phase  $i$ :

$$\begin{aligned} ACR_i(t) &= ACR(t - t_{i-1}), \quad 0 \leq t < t_i, \\ Q_i(t) &= Q(t - t_{i-1}), \quad 0 \leq t < t_i, \end{aligned}$$

where  $t_i$  is the time when Phase  $i$  terminates. Furthermore, the length of Phase  $i$  is defined by  $t_{i-1,i} = t_i - t_{i-1}$ .

Each source end system transmits an RM cell followed by data cells at time 0. Until it receives the first RM cell, its  $ACR$  is decreased exponentially. At time  $\tau_{sx}$ , the RM cells arrive at the switch. At this time, the switch is not congested, and the RM cells will be returned to the source. In actual, it takes one cell time for the switch to handle each RM cell. Then, it may be queued up during processing RM cells when the number of connections is large. However, we assume that all RM cells from sources are transferred simultaneously by the switch. Since the queue length is 0 at time  $\tau_{sx}$ , all sources will increase  $ACR$

at time  $\tau_{sx} + \tau_{xds} = \tau$  by receiving the first backward RM cell. The next phase is determined by the relation between  $ICR$  and  $BW/N_{VC}$ . Type II ( $ACR_{io}(t)$ ) appears when  $N_{VC}ICR < BW$  (Fig. 1), and Type III if  $N_{VC}ICR < BW$ . In what follows, we first derive  $ACR_d(t)$ ,  $ACR_{iu}(t)$  and  $ACR_{io}(t)$ . Then, evolution of  $ACR(t)$  and  $Q(t)$  is shown by determining the length and the initial value of each phase.

The derivation of  $ACR(t)$  and  $Q(t)$  has already been presented in [1]:  $ACR_d(t)$ ,  $ACR_{io}(t)$  and  $ACR_{uo}(t)$  correspond to  $ACR_1(t)$ ,  $ACR_2(t)$  and  $ACR_3(t)$  in [1], respectively. Refer to [1] for more details.

## 2) Evolution of $ACR(t)$ and $Q(t)$ :

In this subsection,  $ACR(t)$  and  $Q(t)$  are derived by taking the same approach presented in [1]. In what follows, we present derivation in the case of  $ICR < BW/N_{VC}$  due to lack of space.

### • $ICR < BW/N_{VC}$

In this case,  $ACR$  is decreased until the first RM cell is returned to the source end system at  $t = \tau$ . Therefore,

$$\begin{aligned} t_1 &= \tau \\ ACR_1(t) &= ACR_d(t), \quad 0 \leq t \leq t_1, \\ Q_1(t) &= 0, \quad 0 \leq t \leq t_1 + \tau_{sx}, \end{aligned}$$

where the initial value of  $ACR_1(t)$  is  $ICR$ .  $ACR$  is then increased until reaching at the value  $BW/N_{VC}$ .

$$\begin{aligned} ACR_2(t) &= ACR_{iu}(t), \quad 0 \leq t \leq t_{12}, \\ Q_2(t) &= 0, \quad \tau_{sx} \leq t \leq t_{12} + \tau_{sx}. \end{aligned}$$

The time  $t_{12}$  is given by as

$$t_{12} = ACR_2^{-1}(BW/N_{VC}) + \tau$$

During Phase 3, the queue length grows and RM cells are returned with a fixed interval  $N_{VC}N_{RM}/BW$  and  $ACR$  is increased according to  $ACR_{io}(t)$ .

$$\begin{aligned} ACR_3(t) &= ACR_{io}(t), \quad 0 \leq t \leq t_{23} \\ Q_3(t) &= \int_{x=\tau_{sx}}^t (N_{VC} ACR_3(x - \tau_{sx}) - BW) dx, \\ &\quad \tau_{sx} \leq t \leq t_{23} + \tau_{sx}. \end{aligned}$$

where  $t_{23}$  is a solution of

$$Q_3(t_{23}) = Q_H.$$

In what follows, we will use the convention  $t_{23} = Q_3^{-1}(Q_H)$  for brevity. After the queue length reaches the threshold value  $Q_H$ ,  $ACR$  is again decreased.  $ACR$  is then increased when  $Q$  becomes the lower threshold value  $Q_L$ .

Last, we note that for later phases, the steady state analysis presented in [1] can be applied.

### 3) Maximum Queue Length:

In this subsection, we show the maximum queue length for  $ICR < BW/N_{VC}$ .

### • $ICR < BW/N_{VC}$

As shown in Fig. 1,  $Q(t)$  reaches at its maximum value during Phase 4. Let the queue length take its maximum value  $Q_{max}$  at  $t_{max}$ . Then, we have a relation

$$\begin{aligned} Q_{max} &= Q^{-1}(t_{max}) \\ t_{max} &= ACR^{-1}(BW/N_{VC}) + \tau_{sx} \end{aligned}$$

### 4) Numerical Examples:

In this subsection, some numerical examples for the EFCI switch are provided. In these examples, both  $Q_H$  and  $Q_L$  are identically set to 500, and other control parameters are set to the suggested values shown in [7].

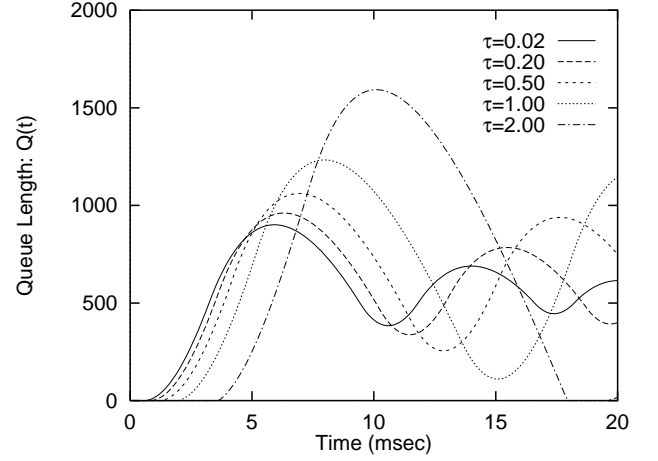


Fig. 2: Effect of Propagation Delay on  $Q(t)$  in EFCI Switch ( $N_{VC} = 10$ ).

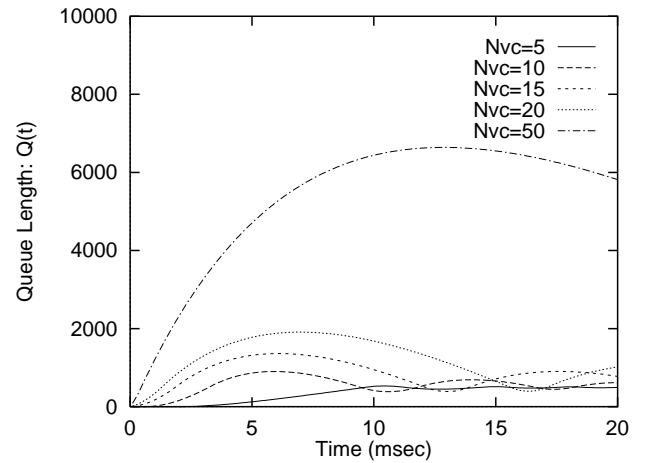


Fig. 3: Effect of  $N_{VC}$  on  $Q(t)$  in EFCI Switch ( $\tau = 0.02$  msec).

The effects of the propagation delays on  $Q(t)$  are displayed in Fig. 2 for  $N_{VC} = 10$ . Since a larger value of  $\tau$  causes slower congestion notification, the queue length is built up initially. Therefore, it is hard to directly apply EFCI switches in the case where we interconnect LANs located in the long distance. After then, the queue length is cyclically fluctuated.

Figure 3 shows  $Q(t)$  for different values of  $N_{VC}$ . The propagation delay between the source and destination end systems are set to be 0.05 ms (around 2 km) as a typical value for a LAN environment. It is obvious that the large  $N_{VC}$  causes an increase of the maximum queue length even in the case of short propagation delays.

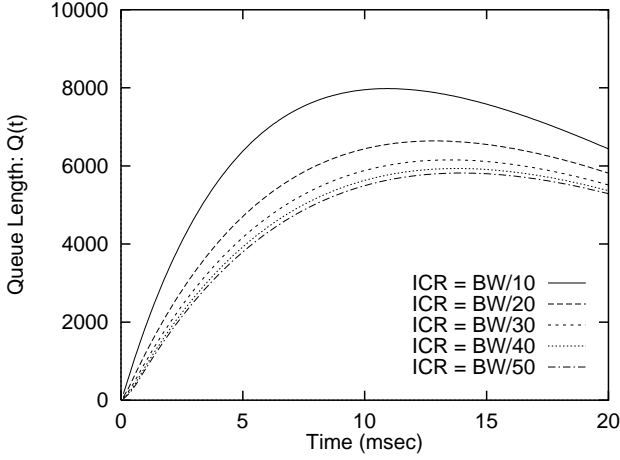


Fig. 4: Effect of Initial Transmission Rate on  $Q(t)$  in EFCI Switch ( $N_{VC} = 50$ ).

A possible solution for decreasing the maximum queue length is to set  $ICR$  properly. In Fig 4, the different values of  $ICR$  are used in the case where  $N_{VC} = 50$  and  $\tau = 0.02$ . As can be seen in the figure, appropriate  $ICR$  can decrease the maximum queue length to some extent. However, it requires to know the active number of connections,  $N_{VC}$ , in advance. If it is difficult to estimate it, we need (1) faster congestion notification achieved by the BES switch which will be presented in the next section, or (2) explicit rate reduction by EDS switch in Subsection III-C.

## B. BES Switch

### 1) Analysis:

In our current model, the analysis for EFCI switches obtained in Subsection III-A can be directly applied to the BES switch by replacing the parameter  $\tau_{xds}$  with  $\tau_{sx}$ . In the BES switch, when the queue length is between  $Q_H$  and  $DQT$ , the congestion notification is selectively performed using  $MACR$ . Therefore, if  $MACR$  is started with a small value at time 0, congestion is notified to the source end system if the queue length exceeds  $Q_H$  according to the control algorithm. However, in the current study, we want to estimate the upper bound of maximum queue length in the initial transient state. Thus, we assume that  $MACR$  is started with a rather large value so that the source end system is not notified of congestion even when the queue length becomes  $Q_H$ . This situation takes place when a number of connections simultaneously starts cell transmission after a single connection has been occupied the link. To avoid this, some mechanism might be required for the BES switch so that if the link is not used during a some period,  $MACR$  is reset to its initial value  $IMR$ .

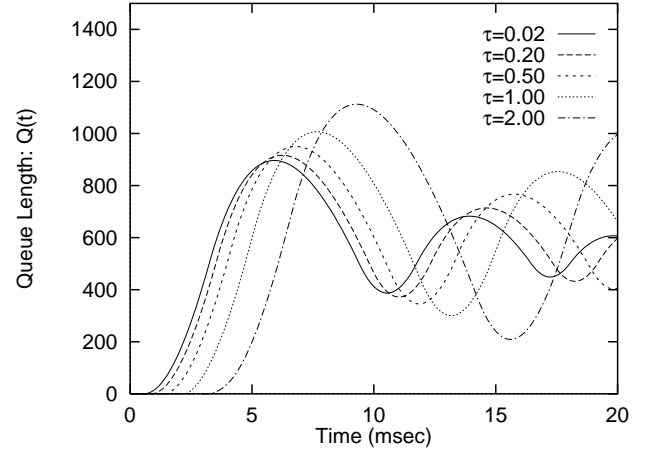


Fig. 5: Effect of Propagation Delay on  $Q(t)$  in BES Switch ( $N_{VC} = 10$ ).

### 2) Numerical Examples:

To see the effect of fast congestion notification of the BES switch, the different values of the propagation delays are used to illustrate Fig. 5. Here the propagation delays  $\tau_{sx}$  (from the source end system to the switch) and  $\tau_{xd}$  (from the switch to the destination end system) are set to be identical. The initial value of  $MACR$ ,  $IMR$ , is set to  $BW$ . As described in the previous subsection, the threshold values  $Q_H$  is not meaningful in the current analysis, and  $DQT$  is set to be 500 which is identical to  $Q_H$  of the EFCI switch. By comparing with Fig. 2 for the EFCI switch, superiority of the BES switch is obvious. For example, the maximum queue length can be decreased from 1700 to 1200 when  $\tau = 2.0$ ms.

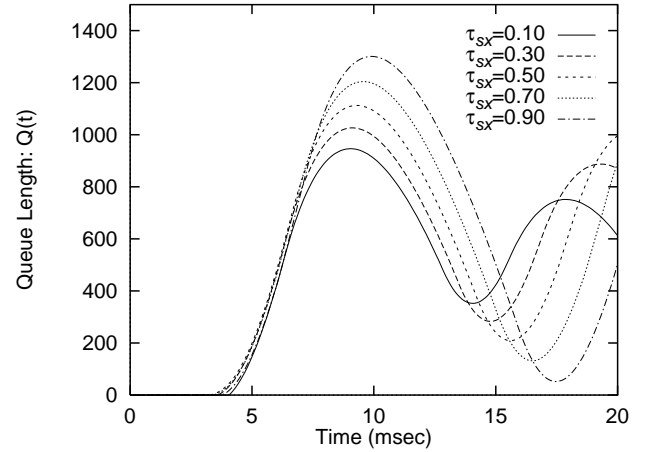


Fig. 6: Effect of Switch Location on  $Q(t)$  in BES Switch ( $N_{VC} = 10$ ).

The location of BES switch affects its performance. Figure 6 shows evolutions of  $Q(t)$  for different  $\tau_{sx}$ 's while the number of connections and the distance between the source and destination end systems are fixed ( $N_{VC} = 10$  and  $\tau_{sx} + \tau_{xd} = 1.0$ ). This result indicates that as the switch is located near the source, the maximum queue length is decreased because of faster conges-

tion notification to the source. However, the BES switch is helpless regarding the large VC's problem. The maximum queue length cannot be decreased even if the BES switch is introduced when  $\tau_{sx}$  is large relative to the end-to-end propagation delay.

### C. EDS Switch

#### 1) Assumptions:

In addition to the assumptions introduced in Section II, the following assumptions are made in analyzing the EDS switch.

(1) The number of connections is large such that  $N_{VC} > BW/ICR$ . The condition  $N_{VC} \leq BW/ICR$  is ideal in the sense that the number of cells initially accumulated at the switch buffer can be eliminated, as has already been shown in EFCI switches. Therefore, we only consider the former condition to investigate the worse case.

(2) Each connection sends a first RM cell at  $t = 0$ . Then, it is followed by data cells. Let  $t'_n$  be the time when the switch processes  $n$ -th forward RM cell sent by the source and carries out EDS operations, i.e., an update of MACR.

$$t'_n = (n-1) \frac{N_{VC}(N_{RM}+1)}{BW} + \tau_{sx}.$$

Here, we assume that RM cells from all sources are processed at time  $t'_n$  while, in actual, it takes one cell time to handle each RM cell. If the queue length is above  $Q_H$ , the estimation using  $MACR$  is performed according to the algorithm. As in the case of the BES switch,  $MACR$  is assumed to begin with a large value. Further, we introduce  $t_n$  which is the time when the source end system possibly receives  $n$ -th RM cell for major rate reduction. Such a case takes place when the switch revives the backward RM cell and the queue length exceeds  $DQT$ .

$$t_n = (n-1) \frac{N_{VC}(N_{RM}+1)}{BW} + \tau,$$

where  $t_0$  is defined as 0.

(3) The rate reduction to  $ER = MACR \times ERF$  does not take place because an initial value of  $MACR$  is large by our assumption.

#### 2) EDS Switch without Priority Control:

In this subsection, we treat the EDS switch without priority control in which the RM cells and data cells are emitted in a FIFO order at the switch.

Before deriving  $ACR(t)$  and  $Q(t)$ , we introduce two additional functions;  $ACR'(t)$  and  $MACR(t)$ . Let  $ACR'(t)$  be  $ACR$  recognized at the switch. This is required because  $ACR(t)$  is the rate of the source at time  $t$ , but due to the queuing delay at the switch,  $ACR$  which the switch recognizes at time  $t$  is not  $ACR(t - \tau_{sx})$ . Actually,  $ACR'(t)$  is given as;

$$ACR'(t) = ACR \left( \frac{BW}{N_{VC}(N_{RM}+1)} (t - \tau_{sx}) \right).$$

Inversely,  $ACR$  of the source end system at time  $t$  is recognized at the switch at time

$$\frac{N_{VC}(N_{RM}+1)}{BW} (t + \tau_{sx}).$$

At time  $t'_n$ , if the queue length is above  $Q_H$ ,  $MACR(t)$  begins to be updated using  $ACR$  contained in the RM cell. We assume that RM cells from the number  $N_{VC}$  of sources are processed at the switch at same time, i.e., the switch calculates  $MACR$  through  $ACR$ 's contained in RM cells from  $N_{VC}$  sources immediately without delay. This assumption gives  $MACR(t)$  as

$$MACR(t'_n) = ACR'(t'_n)(1 - (1 - AV)^{N_{VC}-1}) + (1 - AV)^{N_{VC}} MACR(t'_n -), \quad (1)$$

where  $AV$  is an average factor. Note that  $MACR(t'_n)$  becomes identical to  $ACR'(t'_n)$  when  $N_{VC} = \infty$ . We have  $MACR_n(t)$ , which is defined as  $MACR(t)$  for  $t_n - \tau_{sx} - 2\tau_{xd} \leq t < t_{n+1} - \tau_{sx} - 2\tau_{xd}$  as

$$\begin{aligned} MACR_1(t) &= IMR, \quad 0 \leq t < t_2 - \tau_{sx} - 2\tau_{xd}, \\ MACR_n(t) &= \\ &ACR'(t_n - \tau_{sx} - 2\tau_{xd}) (1 - (1 - AV)^{N_{VC}-1}) \\ &+ (1 - AV)^{N_{VC}} MACR(t_n - \tau_{sx} - 2\tau_{xd}) \\ &n \geq 2, \quad t_n - \tau_{sx} - 2\tau_{xd} \leq t < t_{n+1} - \tau_{sx} - 2\tau_{xd}. \end{aligned}$$

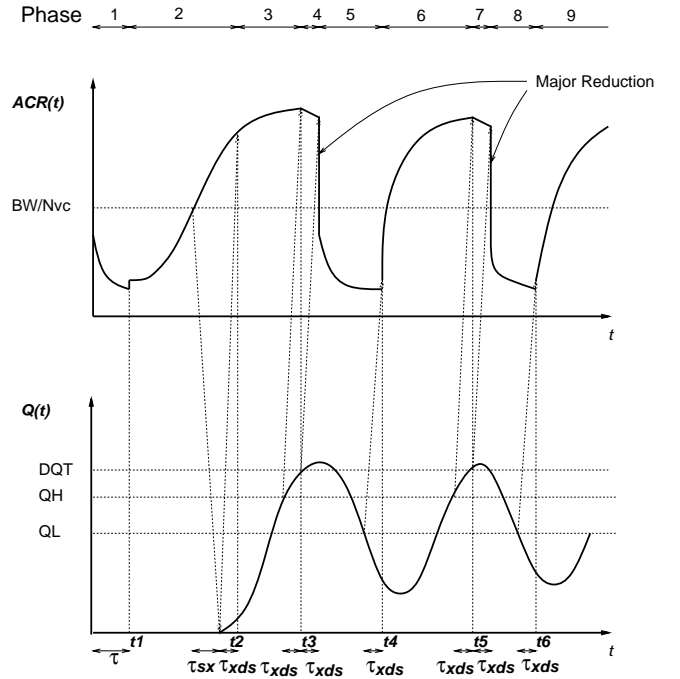


Fig. 7: Pictorial View of EDS Switch with Major Reduction.

Using the above functions, we now obtain  $ACR(t)$  and  $Q(t)$ . Let  $ACR_n(t)$  be  $ACR(t)$  for  $t_n \leq t \leq t_{n+1}$  ( $n \geq 0$ ). Then, we have (see Fig.7)

$$ACR_n(t) = ACR_n(0) e^{-\frac{ACR_n(0)}{MD} (t - t_n)}, \quad t_n \leq t < t_{n+1}$$

where the initial values  $ACR_n(0)$  are given as

$$ACR_0(0) = ICR, \quad (2)$$

$$\begin{aligned}
ACR_1(0) &= \begin{cases} MACR_1(t_n - \tau_{sx}) \times MRF, \\ \text{if } Q_0(t_1 - \tau_{sx}) \geq DQT \\ ACR(2\tau_{sx} + \tau_{xd}) + N_{RM}(AIR + AD R), \\ \text{otherwise} \end{cases} \quad (3) \\
ACR_n(0) &= \begin{cases} MACR_n(t_n - \tau_{sx}) \times MRF, \\ \text{if } Q_{n-1}(t_n - \tau_{sx}) \geq DQT \\ ACR_{n-1}(t_n), \\ \text{otherwise} \end{cases} \quad (4)
\end{aligned}$$

Here, we should take account of possibilities of major rate reduction.

The corresponding queue length is determined as

$$\begin{aligned}
Q_0(t) &= \int_{\tau_{sx}}^t \left\{ \frac{N_{RM} + 1}{N_{RM}} N_{VC} ACR_0(x - \tau_{sx}) - BW \right\} dx, \\
&\quad \tau_{sx} \leq t < t_1 + \tau_{sx}, \\
Q_n(t) &= Q_{n-1}(t_n + \tau_{sx}) \\
&+ \int_{t_n + \tau_{sx}}^t \left\{ \frac{N_{RM} + 1}{N_{RM}} N_{VC} ACR_n(x - \tau_{sx}) - BW \right\} dx, \\
&\quad t_n + \tau_{sx} \leq t < t_{n+1} + \tau_{sx}.
\end{aligned}$$

In the below, we will derive an formula for the queue length just before the first major reduction, which is likely to happen at time  $t_2$  in the case of the large number of  $N_{VC}$ . First the queue length at time  $t_1 + \tau_{sx}$  is given by

$$Q_0(t_1 + \tau_{sx}) = \frac{N_{RM} + 1}{N_{RM}} N_{VC} MD (1 - e^{-\frac{ICR}{MD}\tau}) - BW \tau$$

Then the queue length at time  $t_2 + \tau_{sx}$  is given by

$$\begin{aligned}
Q_1(t_2 + \tau_{sx}) &= Q_0(t_1 + \tau_{sx}) \\
&+ \frac{N_{RM} + 1}{N_{RM}} N_{VC} MD (1 - e^{-\frac{ACR_1(0)}{MD} \frac{N_{VC}(N_{RM}+1)}{BW}}) \\
&- N_{VC}(N_{RM} + 1), \quad (5)
\end{aligned}$$

where  $ACR_1(0)$  was given in (3).

Here, we have assumed that the queue length at time  $t_2 - \tau_{sx} - 2\tau_{xd}$  is beyond  $Q_H$ , and that the queue length at time  $t_2 - \tau_{sx}$  exceeds  $DQT$ . Due to the lack of space, we omit the condition that this case takes place, but it is easily obtained. The condition that the queue length does not increase after  $t_2$  is given by

$$N_{VC} ACR_2(0) \leq BW$$

where

$$ACR_2(0) = MRF ICR e^{-\frac{ICR}{MD} \left(1 + \frac{BW \tau_{sx}}{N_{VC}(N_{RM}+1)}\right)}.$$

As will be shown in the numerical examples, the above queue length does not always give the maximum value at the initial transient state. However, in (5), we have a free design parameter  $MRF$ , and it can prevent the queue length to unacceptably become large.

### 3) EDS Switch with Priority Control:

In this subsection, the prioritized EDS switch is evaluated where the RM cells are given preferential service at the switch via

Head-of-Line priority discipline, i.e., the RM cells are always served if any at the switch buffer. The additional assumptions for the analysis to be tractable are described below.

(1) The bandwidth available to the data cells is given by subtracting the bandwidth for high priority RM cells from the total bandwidth, i.e.,

$$BW \frac{N_{RM}}{N_{RM} + 1}.$$

(2)  $ACR'(t)$  equals to  $ACR(t)$  at time  $t - \tau_{sx}$  because of preferential service to RM cells, that is, the RM cell is processed immediately on its arrival at the switch.

$$ACR'(t) = ACR(t - \tau_{sx})$$

Therefore, we neglect the delay due to contention among RM cells.

(3)  $n$ -th backward RM cell arrives at the switch at time  $t_n = s_n + \tau$  where  $s_n$  satisfies

$$\int_0^{s_n} ACR(t) dt = (n - 1) N_{RM}. \quad (6)$$

That is, we need not take account of queuing delay of RM cells due to its priority service.

The definition of  $ACR(t)$  is just same as in the case of the EDS switch without priority control. The queue length at the switch is then obtained as

$$\begin{aligned}
Q_0(t) &= \int_{\tau_{sx}}^t \left\{ N_{VC} ACR_0(x - \tau_{sx}) - BW \frac{N_{RM} + 1}{N_{RM}} \right\} dx, \\
&\quad \tau_{sx} \leq t < t_1 + \tau_{sx} \\
Q_n(t) &= Q_{n-1}(t_n + \tau_{sx}) \\
&+ \int_{t_n + \tau_{sx}}^t \left\{ N_{VC} ACR_n(x - \tau_{sx}) - BW \frac{N_{RM} + 1}{N_{RM}} \right\} dx, \\
&\quad n \geq 1, \quad t_n + \tau_{sx} \leq t < t_{n+1} + \tau_{sx}.
\end{aligned}$$

If the first major reduction occurs at time  $t_2$ , the queue length at time  $t_2 + \tau_{sx}$  is given as

$$\begin{aligned}
Q_1(t_2 + \tau_{sx}) &= Q_0(t_1 + \tau_{sx}) \\
&+ MD N_{VC} (1 - e^{-\frac{ACR_1(0)t_2}{MD}}) - BW (t_2 - t_1) \frac{N_{RM}}{1 + N_{RM}},
\end{aligned}$$

where

$$Q_0(t_1 + \tau_{sx}) = MD N_{VC} (1 - e^{-\frac{ICR t_1}{MD}}) - BW t_1 \frac{N_{RM}}{1 + N_{RM}}.$$

In the above equation,  $t_2$  is obtained as follows. When  $s_2 \leq \tau$ , the following inequality holds.

$$\int_0^{2\tau_{sx} + \tau_{xd}} ACR_0(t) < N_{RM} + 1.$$

Then  $s_2$  is obtained from the following equation,

$$\int_0^{s_2} ACR_0(t) = MD (1 - e^{-\frac{ICR}{MD} t}).$$

That is,

$$s_2 = \frac{MD}{ICR} \log \frac{MD}{MD - (N_{RM} + 1)},$$

which determines  $t_2$  from (6).

On the other hand, when  $s_2 > \tau$ ,  $s_2$  is given by

$$s_2 = -\frac{MD}{ICR} \log \left\{ \frac{N_{RM} + 1}{MD} - \left( 1 - e^{\frac{ICR}{MD}\tau} + e^{\frac{ACR_1(0)}{MD}\tau} \right) \right\}.$$

If  $ACR$  is not decreased enough to sustain the queue length, the queue length would still grow. In that case, a smaller value of  $MRF$  should be used to decrease the maximum queue length.

#### 4) Numerical Examples:

In this subsection, we provide numerical examples for EDS and PEDS switches. The suggested control parameters in Appendix are used except  $DQT$ ,  $Q_H$  and  $Q_L$ .  $DQT$  is set to 500, and both  $Q_H$  and  $Q_L$  are set to 100 for comparison with EFCI and BES switches.

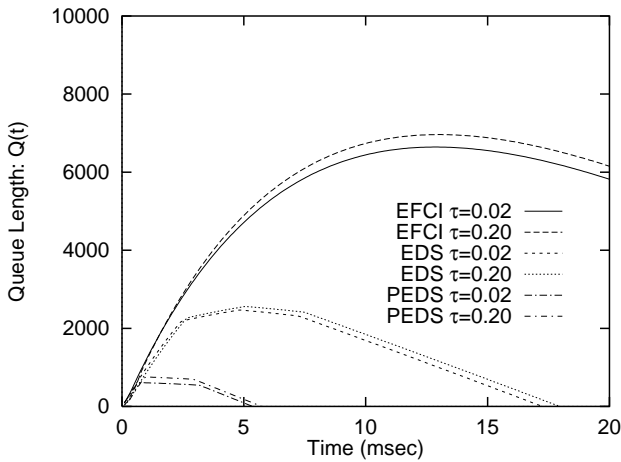


Fig. 8: Initial Evolution of  $Q(t)$  ( $N_{VC} = 50$ ).

Initial evolutions of  $Q(t)$  are plotted in Fig. 8. In this figure,  $N_{VC}$  is set to 50 and  $\tau$  is varied. The case of the EFCI switch is also shown for comparison. The result of the BES switch is not shown because it is almost same as the one of the EFCI switch. It is remarkable that giving priority to RM cells in the PEDS switch can drastically decrease the maximum queue length.

In Fig. 9, the maximum queue length in the EDS switch for different values of  $N_{VC}$ 's are plotted. The increase of  $N_{VC}$  affects the maximum queue length directly while the propagation delay has little influence on it. The number of connections,  $N_{VC}$ , is still a major dominant factor for the maximum queue length even in the case of the EDS switch. On the contrary, the influence of  $N_{VC}$  on the maximum queue length becomes less in the PEDS switch. For example, the required buffer for PEDS switch becomes less than 3000 cells even if  $\tau = 2.0$  (about 200 km) and  $N_{VC} = 100$ . In the case of EFCI and EDS switches, the corresponding values are 18,000 and 14,000, respectively. Consequently, the PEDS switch can be valuable to be implemented even though it requires an additional control complexity.

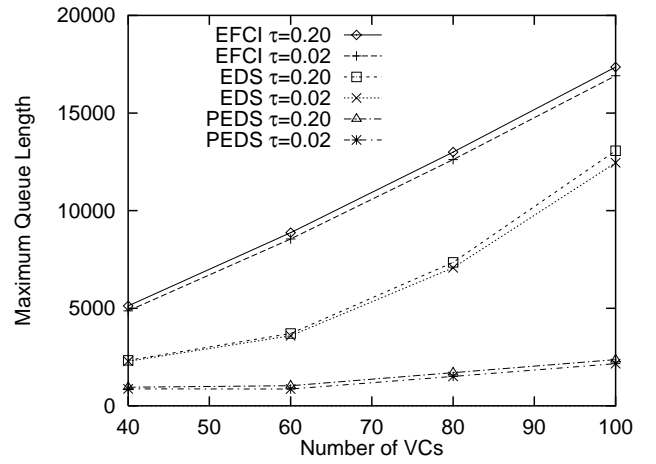


Fig. 9: Effect of  $N_{VC}$  on Maximum Queue Length.

## IV. CONCLUDING REMARKS

For further works, some mechanism to estimate the initial cell rate appropriately according to the number of active connections should be investigated. In general, it is not easy to know the number of active connections in advance. However, an appropriate signalling protocol may realize such a mechanism.

## REFERENCES

- [1] H. Ohsaki, M. Murata, H. Suzuki, C. Ikeda, and H. Miyahara, "Analysis of rate-based congestion control methods in ATM networks — part 1: Steady state analysis —," *to be presented at GLOBECOM '95*, 1995.
- [2] H. Ohsaki, M. Murata, H. Suzuki, C. Ikeda, and H. Miyahara, "Rate-based congestion control for ATM networks," *ACM SIGCOMM Computer Communication Review*, vol. 25, April 1995.
- [3] J.-C. Bolot and A. U. Shankar, "Dynamical behavior of rate-based flow control mechanisms," *Computer Communication Review*, vol. 20, pp. 35–49, 4 1990.
- [4] K. K. Ramakrishnan and R. Jain, "A binary feedback scheme for congestion avoidance in computer networks," *ACM Transactions on Computer Systems*, vol. 8, no. 2, pp. 158–181, 1990.
- [5] N. Yin and M. G. Hluchyj, "On closed-loop rate control for ATM cell relay networks," *IEEE INFOCOM '94*, pp. 99–109, June 1994.
- [6] J. C. R. Bennett and G. T. D. Jardins, "Failure modes of the baseline rate based congestion control plan," *ATM Forum Contribution 94-0682*, July 1994.
- [7] L. Roberts, "Enhanced PRCA (proportional rate-control algorithm)," *ATM Forum Contribution 94-0735R1*, August 1994.